This article was downloaded by: [University of Haifa Library]
On: 11 August 2012, At: 10:59
Publisher: Taylor & Francis
Informa Ltd Registered in England and Wales Registered Number: 1072954
Registered office: Mortimer House, 37-41 Mortimer Street, London W1T 3JH, UK

Molecular Crystals and Liquid Crystals

Publication details, including instructions for authors and subscription information:
http://www.tandfonline.com/loi/gmcl20

Time Evolution of Director Patterns in Rotating Nematic Samples

Alexandre Escalhão Gomes [a] , Antonino Polimeno [a] , Laura Orian [b] & Assis Farinha Martins [b]

[a] Dipartimento di Chimica Fisica 'A. Miolati', Università degli Studi di Padova, Via Loredan 2, Padova, 35131, Italy

[b] Departamento de Ciência dos Materiais, Faculdade de Ciência e Tecnologia, Universidade Nova de Lisboa, Caparica, 2829-516, Portugal

Version of record first published: 18 Oct 2010

To cite this article: Alexandre Escalhão Gomes, Antonino Polimeno, Laura Orian & Assis Farinha Martins (2003): Time Evolution of Director Patterns in Rotating Nematic Samples, Molecular Crystals and Liquid Crystals, 395:1, 295-310

To link to this article: http://dx.doi.org/10.1080/15421400390193837

PLEASE SCROLL DOWN FOR ARTICLE

Full terms and conditions of use: http://www.tandfonline.com/page/terms-and-conditions

This article may be used for research, teaching, and private study purposes. Any substantial or systematic reproduction, redistribution, reselling, loan, sub-licensing, systematic supply, or distribution in any form to anyone is expressly forbidden.

The publisher does not give any warranty express or implied or make any representation that the contents will be complete or accurate or up to date. The accuracy of any instructions, formulae, and drug doses should be independently verified with primary sources. The publisher shall not be liable for any loss, actions, claims, proceedings, demand, or costs or damages whatsoever or howsoever caused arising directly or indirectly in connection with or arising out of the use of this material.

Downloaded by [University of Haifa Library] at 10:59 11 August 2012

Mol. Cryst. Liq. Cryst., Vol. 395, pp. [295]/125–[310]/140, 2003
Copyright © Taylor & Francis Inc.
ISSN 1542-1406 print/1563-5287 online
DOI: 10.1080/15421400390193837

Taylor & Francis
Taylor & Francis Group

TIME EVOLUTION OF DIRECTOR PATTERNS IN ROTATING NEMATIC SAMPLES

Alexandre Escalhão Gomes and Antonino Polimeno
Dipartimento di Chimica Fisica 'A. Miolati', Università degli Studi di Padova, Via Loredan 2, 35131 Padova Italy

Laura Orian and Assis Farinha Martins
Departamento de Ciência dos Materiais, Faculdade de Ciência e Tecnologia,Universidade Nova de Lisboa, 2829-516 Caparica Portugal

Downloaded by [University of Haifa Library] at 10:59 11 August 2012

In this paper, constitutive hydrodynamic equations are numerically solved for a nematic liquid crystal in a cylindrical sample rotating around its axis at a constant angular velocity and subject to a magnetic field. The computational solution of the problem is achieved in three dimensions by uncoupling the velocity and the director fields, and assuming the velocity field of a classical Newtonian fluid. The influence of initial and boundary conditions is considered. The formation and time evolution of patterns is calculated and discussed in terms of average behaviour and spatial distributions, which give evidence of the complex local behaviour of the nematic director.

Keywords: nematic liquid crystals; hydrodynamics; director patterns

INTRODUCTION

The complex hydrodynamic behaviour of a nematic liquid crystalline system can be described by two vector fields depending upon space and time t [1,2]: the director unit vector $\mathbf{n} = (n_1, n_2, n_3)$, which describes the local orientation of the mesogenic phase, and the velocity vector $\mathbf{v} = (v_1, v_2, v_3)$. Leslie [3] and Ericksen [4] first derived the constitutive equations that describe the time evolution of incompressible isothermal nematic fluids, i.e. the nematic hydrodynamic behaviour for some defined initial and boundary conditions.

This work was partly supported by the European Commission under TMR contract FMRX-CT97-0121 and by the Italian Ministry for Universities and Scientific and Technological Research (PRIN "Cristalli Liquidi")

Downloaded by [University of Haifa Library] at 10:59 11 August 2012

Applications of Leslie-Ericksen (LE) equations to the analysis of dynamical behaviour of nematics have been increasingly spread in the scientific community, both in the form of simplified analytical treatments and complete numerical solutions. This is due to the necessity of describing advanced experimental set-ups, which are based on standard rheological set-ups (Couette, cone-and-plate geometries etc.) with magnetic or optical spectroscopies, or combination of different experimental techniques, which can give information on the visco-elastic behaviour of a liquid crystalline phase in the course of few combined magneto-rheological or optical-rheological experiments. Comparison with analytical predictions of LE theory is also considered usually a benchmark test for refined theoretical treatments. Finally advanced numerical approaches based on LE equations are made relatively easier with the continuously increasing advance of computational fluid dynamics.

Recent applications of LE equations and theory are due to several workers. Numerical solutions of LE equations with or without applications to the interpretation of rheological experiments have been conducted recently by Rey, who has obtained numerical solution to LE equations for the creeping flow of a low molar mass nematic between concentric parallel disks [5]. Kneppe, Schneider *et al*. have treated the flow of a nematic fluid around a spherical and cylindrical object [6]. A finite-element approach has been used for treating LE equations in complex geometries, under simplifying hypotheses and in two-dimensions, by Baleo, Vincent *et al*. [7]. Han and Rey have conducted a numerical analysis of LE equations for rectilinear shear flows in low molar mass nematics and nematic liquid crystalline polymers [8]. Non-isothermal Poiseuille flow of nematic fluids have been described using LE equations by Potze and Heynderickx [9]. Chan and Rey have discussed a synthesis of LE theory and Euler-Lagrange equations for treating the reorientational dynamics in bipolar nematic droplets [10]. Chono, Tsuji and Denn have described the development of director patterns in tumbling nematics for two-dimensional flow between parallel plates [11]. Chan has conducted computer simulations of bipolar nematic droplets by solving numerically LE equations [12].

Liquid crystalline polymers have been an interesting object of application of LE theory. Berry and Srinivasaro have used LE constitutive equations to discuss the rheological properties of nematic solutions of rod-like polymers [13]. The role of director tumbling in the dynamic response of polymer liquid crystals have been investigated by Burghardt and Fuller using LE theory [14]. Larson and Doi have employed a mesoscopic treatment of textured sample of liquid crystalline polymers based on spatially averaged LE equations [15]. Marrucci has considered the application of a LE approach to tumbling motion in flow experiments carried on in nematic liquid crystalline polymers [16]. Chang, Shiao and Yang have studied two-dimensional flows in nematic polymers via simplified LE theory [17].

Downloaded by [University of Haifa Library] at 10:59 11 August 2012

Optical and electro-rheological experiments have also profited from approaches based on LE theory. Interpretation of micro-dielectric measurements in flowing nematic liquid crystals has been conducted by Fodor and Hill using LE theory [18]. Rheo-optical investigations of flow properties of nematic liquid crystals have been interpreted using LE equation by Muller, Stein and Winter [19]. Bajc, Hillic and Saupe have analyzed conductivity measurements of elastic constants and rotation viscosity of micellar liquid crystals using LE theory [20]. Mather *et al.* [21] have discussed the origin of oscillation damping optically observed in torsional shearing of nematics using LE equations. Molecular precession induced by shear in Langmuir monolayers have been described quantitatively using LE theory by Ignes-Mullol and Shwartz [22].

Application of Leslie-Ericksen (LE) theory to the interpretation of rheological experiments can be highly profitable since it provides a direct way to determine the viscous and elastic parameters defining the nematic fluid mechanical properties. However, numerical analysis based on LE formalism is usually rather complex, unless drastic simplifying hypotheses are made. In this work we present a careful numerical analysis of director patterns predicted by the LE equations for a well known and relatively simple geometry, namely a cylindrical sample rotating at constant angular velocity around its symmetry axis, taking into account the full spatial dimensionality of the problem. The sample is subject to the action of a constant, uniform magnetic field applied in the plane perpendicular to the rotation axis. Cylindrical set-ups have been and are common in rheological experiments performed on liquid crystals, since the seminal experiments performed by Tsevtkov [23], Leslie *et al.* [24], Emsley *et al.* [25], and Kneppe and Schneider [26]. Rheological and Rheo-Nuclear Magnetic Resonance (NMR) experiments in similar geometries, involving step rotations of the sample combined with magnetic fields, have been conducted, among others, by Martins and co-workers, to obtain the viscoelastic parameters of the nematic phase [27]. More recently a series of theoretical studies on the solution of LE equations, both by semi-analytical [28] and by numerical [29] methods, have been conducted by Polimeno, Martins and co-workers always assuming that both the director and velocity fields are constrained to lie in a planar section of the sample, i.e. for bi-dimensional geometries.

In this work we consider a full three-dimensional description of the director field in space, and study numerically how different initial conditions and rotational velocities can influence the time evolution of the nematic director patterns in space. We assume the only basic approximation that the velocity field for a low viscous nematic can be described by a Newtonian behaviour [30], allowing the uncoupling from the director field, and thus simplifying the numerical solution of the LE equation for the director orientation in space. The article is organised as follows. In the next

Section we briefly summarise the numerical algorithm employed in the solution of LE equations. A presentation of our results is then given. Finally a brief discussion of the main findings is given in the last Section.

THE MODEL

Let us consider a Cartesian frame $\mathbf{e_1}, \mathbf{e_2}, \mathbf{e_3}$ as defined in Figure 1. Leslie-Ericksen equation for i-th director field component n_i can be written in explicit form as

$$\frac{\partial n_i}{\partial t} = \lambda n_i + \frac{\Delta\chi B_j n_j B_i}{\mu_0 \gamma_1} - v_j n_{i,j} + \frac{1}{2}\left[\left(v_{i,j} - v_{j,i}\right) - \frac{\gamma_2}{\gamma_1}\left(v_{j,i} + v_{i,j}\right)\right] n_j + \frac{K}{\gamma_1}\nabla^2 n_i \tag{1}$$

where $n_{i,j}$ stands for the r$_j$ spatial derivative of n_i, λ represents a Lagrange multiplier, related to the usual constraint $n_i n_i = 1$; B_i is the i-th component of the imposed magnetic field, v_i the velocity field component. Einstein's summation convention is used everywhere in the paper, if not stated otherwise. For the sake of simplicity we assume a spherical approximation for the elastic tensor $K_1 = K_2 = K_3 = K$ [1,2]: thus the viscosity coefficients γ_1 and γ_2 and the average elastic constant K are the only characteristic viscoelastic parameters of the nematic which are taken in consideration. The director field equations are accompanied by velocity field equations which govern the time and space variation of v_i: they

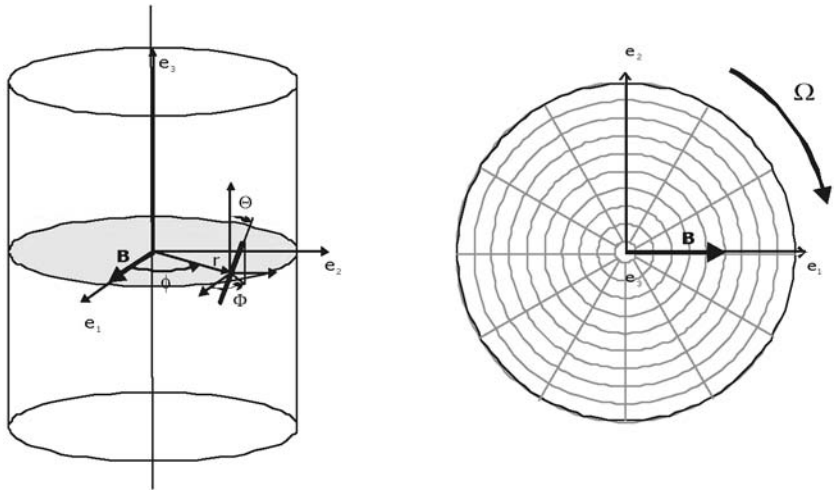

FIGURE 1 Geometrical setup.

Downloaded by [University of Haifa Library] at 10:59 11 August 2012

describe the hydrodynamic behaviour of the nematic fluid, essentially including the influence of the anisotropic medium in the standard Navier-Stokes formulation. The computational problem posed by the full solution of LE equations both with respect to v_i and n_i is of considerable difficulty and has been discussed recently in two dimensions employing a streamline function-vorticity approach [9].

Here we wish to explore the time evolution of director patterns assuming a full three-dimensional description for the director, i.e. all three components are considered explicitly, but within the following approximations: 1) spatial bi-dimensionality of the coordinate space, i.e. we consider an infinitely long cylindrical sample for which translation invariance is valid, therefore **n** does not depend upon r_3 and 2) Newtonian stationary velocity field, i.e. the velocity field is described by the analytical expression for a Newtonian fluid undergoing constant rotation at an angular velocity **Ω**, so that for a cylinder rotating around axis $\mathbf{e_3}$ the velocity field is simply given by $\mathbf{v} = \mathbf{r} \times \mathbf{\Omega e_3}$.

The Newtonian velocity approximation is rather severe for the case of sudden rotation of the nematic sample, when the fluid is set in motion or when the sample is suddenly arrested after rotation. Detailed studies of Electron Spin Resonance measurements (ESR) performed on low molecular weight nematics subject to sudden rotation give evidence of strong non-Newtonian behaviour due to the influence of director dynamics on the velocity in the form of backflow effect [31]. However, here we are interested only in the patterns formed by the director well after the transient initial regime of rotation, for a sample in continuous rotation at relatively low values of the angular velocity. To this purpose, we consider an infinitely long tube of radius R, and we solve numerically Eq. (1) in a planar section. The geometry and the reference frame are shown in Figure 1. The sample is subject to a constant magnetic field applied along the $\mathbf{e_1}$ axis, i.e. $\mathbf{B} = B\mathbf{e_1}$ and to a constant rotation with angular velocity **Ω**. Boundary and initial conditions for the director need still to be defined. Their choice can affect considerably the director time evolution and the formation of stable or unstable spatial patterns. We assume for simplicity that the surface imposes a preferential orientation to the director, in a regime of infinite anchoring strength [1,2] where the director at the surface is oriented in the plane along the radius. In the following, we shall summarise these conditions as *radial boundary conditions*, RBC. For the case of untreated tube probes real experimental conditions are likely to favour weak anchoring conditions. The treatment of weakly anchored systems is analogous and has been presented elsewhere, although the patterns predicted for the director can be significantly more complex, especially at high angular velocity [1]. Notice that for RBC we can write for the director components on the boundary $\mathrm{n}_1 = \cos\phi, \mathrm{n}_2 = \sin\phi, \mathrm{n}_3 = 0$, where ϕ is the angular polar coordinate (cf. Fig. 1).

Downloaded by [University of Haifa Library] at 10:59 11 August 2012

Downloaded by [University of Haifa Library] at 10:59 11 August 2012

Initial conditions are chosen by assuming that the director is distributed at $t = 0$ according to a stable distribution resulting from elastic and magnetic torques, and boundary conditions alone. We shall discuss in this work the time evolution of the director field starting from two different initial conditions, corresponding to two possible stable configurations of the still sample in the presence of the magnetic field and subject to RBC. Let us first briefly discuss director configurations in the absence of the magnetic field. According to Cladis [32] and Ondris-Crawford [33] nematic liquid crystals confined in circular cavities can assume what is called a planar polar (PP) structure, i.e. the director is homogeneously distributed in the sample with zero component along the cylinder axis. Radial distributions are also possible and for radii larger than 0.1 μm an escaped-radial (ER) structure is observed, i.e. the director assumes a radial distribution with the formation of a disclination line along the cylinder axis. We assume in the following that our sample, initially prepared either in a PP or in an ER configuration, is left still in the presence of the magnetic field long enough to reach a stable structure. We therefore take as initial conditions in the absence of magnetic field that the director is either homogeneously distributed along the $\mathbf{e_1}$ axis, i.e. $n_1 = 1, n_2 = 0, n_3 = 0$ (PP) or along the radial direction in the whole sample, with an out-of-plane angle distribution given by $\alpha = 2 \cdot \text{atan}\,(R/r) - \pi/2$, i.e. $n_1 = \cos\phi\cos\alpha, n_2 = \sin\phi\cos\alpha, n_3 = \sin\alpha$ (ER) everywhere in the bulk. The magnetic field has the effect of inducing a distortion on the chosen stationary distribution and this is taken into account numerically, by allowing the simulated nematic to adjust to the magnetic torque (see next Section).

RESULTS

In order to calculate numerically the time evolution of the director patterns in the sample, we employ a straightforward finite difference algorithm to discretize Eq. (1) in space, by using a polar grid (check Fig. 1). For instance, in a typical simulation a grid of 20 points per radius and 40 per angle is employed, for a total of 800 internal points. At each point of the spatial grid, the derivatives of the three director components are calculated at each time step and the new director components are evaluated using a modified Crank-Nicholson scheme, which takes into account the constraint of unitary vector, imposed upon $\mathbf{n}$. Simulations conducted on a Silicon Graphics Octane take on average 5 hours of CPU time per 50 seconds of simulation time. The system is prepared initially either in a PP or in a ER configuration, and is left still ($\mathbf{\Omega} = 0$) for a time long enough to allow the formation of a stationary distribution under the influence of the magnetic field, usually 50 to 100 seconds (*equilibration*). The new stationary dis-

Downloaded by [University of Haifa Library] at 10:59 11 August 2012

tribution is assumed as the true initial director distribution at $t = 0$, before the rotation begins. Notice that at this stage (*acceleration*) the angular velocity imposed to the tube is increased linearly from 0 to Ω in a time which has been chosen equal to 1 s for all simulations.

The starting distribution for dynamical simulation shows, naturally, a region where the director has a distorted configuration going from the alignment with the wall to the alignment with the magnetic field, with a typical magnetic coherence length $\xi(B) = \sqrt{K\mu_0/\Delta\chi B^2}$ that gives the thickness of this transition layer [1,2].

Patterns obtained for the system in rotation are far more complex. According to a simple analysis based on neglecting the spatial dependence of the director [1,2], when the system is set in rotation the existence of two dynamical regimes can be predicted, depending on the velocity imposed to the cylinder: below a critical velocity

$$\Omega_c = \Delta\chi B^2/2\gamma_1\mu_0 \tag{2}$$

the director assumes a stationary orientation at an absolute equilibrium angle given by

$$2\phi_c = \arcsin \Omega/\Omega_c \tag{3}$$

Above the critical velocity Ω_c it is easily predicted [1,2] that the director does not reach a stable orientation, but rotates in time, with an effective frequency given by

$$\Omega_{eff} = \sqrt{\Omega^2 - \Omega_c^2} \tag{4}$$

However the complete numerical solution shows that the actual situation can be considerably more complicated than the one predicted by an analytical solution, and that the formation of unstable dynamical regime patterns is involved. We can still maintain however, at least as a guideline, the general distinction between dynamical regimes simulated below and above the critical velocity Ω_c, which we may assume to be a rough criterion for discriminating between the formations of stationary or non-stationary director patterns.

We choose as a prototype sample for our simulations p-methoxybenzylidene-p′-n-butylaniline (MBBA) for which complete set of viscoelastic parameters is available in literature, and which has a positive value of the anisotropic diamagnetic susceptibility $\Delta\chi$. Naturally, quite different behaviour can be expected from a nematogen with $\Delta\chi < 0$. The viscoelastic and magnetic parameters of MBBA are reported in Table 1 [29]. The intensity of the applied magnetic field is typical of an X-bound ESR experiment, 0.33 T. For MBBA, using this value of the magnetic field, we estimate a value of the critical velocity $\Omega_c = 0.0867$ Hz, and a magnetic

TABLE 1 Viscoelastic Parameters for N-(p-methoxybenzylidene)-p butylaniline(MBBA) 10K Below its Clearing Point

Anisotropic diamagnetic susceptibility $\Delta\chi$	1.0×10^{-7}
Viscosity coefficients α_i (Pa s^{-1})	−0.0087; −0.052; −0.002; 0.058; 0.038; −0.016
Average elastic constant K (N)	5.3×10^{-11}
Magnetic flux density B (T)	0.33

coherence length of 0.758×10^{-4} m. We present simulations for samples having a fixed radius of 1.0×10^{-3}m, for both PP and ER structures.

To illustrate the complexity of dynamical behaviour exhibited by the director, we start to show in Figure 2 three-dimensional snapshots of the director patterns in the absence of rotation (still sample). Here and in the following figures we represent the director as a thin rod, and we show the director behaviour only in a limited number of points, corresponding to a rarefied grid of 10 by 20 points, for clarity of representation. Snapshots group (a) shows the initial and final steady state conformation of the director for an initial PP structure and group (b) shows the same conformations corresponding to a ER structure. In both cases the stationary

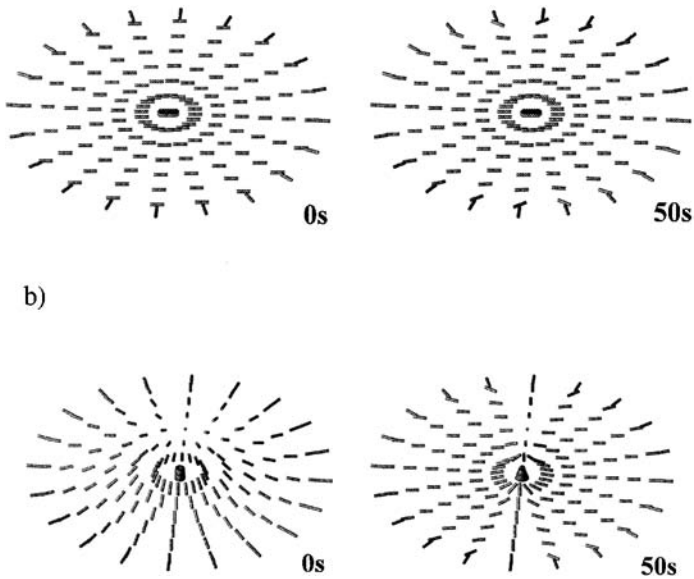

FIGURE 2 3-D snapshots of the director orientation at stationary state at $\Omega = 0$, for the cases of PP initial configuration (a) and ER initial configuration (b).

Downloaded by [University of Haifa Library] at 10:59 11 August 2012

distribution resulting from the application of the magnetic field (which is arbitrary taken at 50 s although practically no changes are observed already after 1 s of simulation) shows a characteristic alignment with the $\mathbf{e_1}$ direction, along the magnetic field. In the case of a starting ER structure, the application of the magnetic field naturally destroys the initial axial symmetry, as most of the sample aligns with the field, but the central region aligned along the cylinder axis is kept.

Polar Planar (PP) Case

We start to comment the dynamical evolution in time of director patterns from a distorted PP distribution (in the following we shall simply write PP sample or case). In Figure 3 we represent the time evolution of the rotating PP sample for the different rotational velocities: $\Omega = \Omega_c/2$ (a), $\Omega = \Omega_c$ (b), $\Omega = 5\Omega_c$ (c) at 20, 40 and 100 s. In the three cases we observe that the director forms essentially homogeneous distributions, which are kept in the plane, not surprisingly, since the deterministic LE equations in the limit of Newtonian velocity field do not provide torques able to favour the escape of the director field along the third direction. Director patterns generated for rotational velocity smaller than the critical velocity given by Eq. (2), case (a), or equal to the critical velocity, case (b), reach a stationary distribution, while for a higher value, case (c), the director exhibits a non-stationary distribution, which is homogenous except for an annulus close to the border subject to RBC.

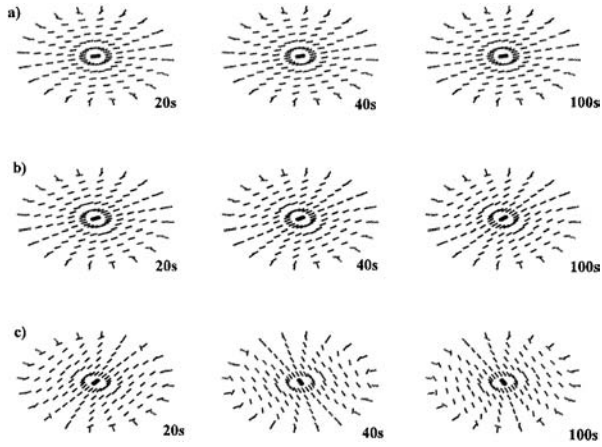

FIGURE 3 3-D snapshots of the director orientation at different rotational velocities for a PP sample, velocities $\Omega = \Omega_c/2$ (a); $\Omega = \Omega_c$ (b) and $\Omega = 5\Omega_c$ (c).

Downloaded by [University of Haifa Library] at 10:59 11 August 2012

Downloaded by [University of Haifa Library] at 10:59 11 August 2012

We can describe quantitatively the director distribution director orientation by introducing proper averages extended to the whole sample. In general the director Cartesian components are given in terms of polar angles $n_1 = \cos\Phi \sin\Theta$, $n_2 = \sin\Phi \sin\Theta$, $n_3 = \cos\Theta$; we define average angles $\langle\Phi\rangle$ and $\langle\Theta\rangle$ where $\langle\ldots\rangle$ is the integral extended to the circular region, divided by its area πR^2 for normalization; thus $\langle\Phi\rangle$ and $\langle\Theta\rangle$ are the azimuthal and polar average director angle. In the following we shall also need the angle between the director and the magnetic field $\Phi_B = \arccos n_1$, simply defined as the arccosine of the first director component since the field has been taken along the $\mathbf{e_1}$ axis. In the present PP case $\Theta = 0$ and $\Phi = \Phi_B$. In Figure 4 the average azimuthal angle is shown for the three cases; for comparison the case of zero velocity is also included, corresponding to $\langle\Phi\rangle = 0$. The stable configurations reached in cases (a) and (b) correspond to a stationary average azimuthal angle with an absolute value which is significantly smaller than the value predicted in each case by Eq. (3): 11° vs. 15° in case (a) and 33° vs. 45° in case (b), due to the influence of boundary conditions. In case (c) oscillations of the average azimuthal angle are observed with a period roughly equal to 7 s, to be compared to the value of 6.2 s predicted by standard theory. On the whole the simplified description provided by Eq. (2), (3) and (4) is respected. Notice however that this is strictly true only if average values of the director field components (or angles) are considered. A more careful analysis of the actual patterns obtained from the simulations proves that the director angle, Φ, always exhibits a distribution of values. In Figure 5 we show histograms relative to patterns reached for cases (a), (b) and (c), plus the case of zero

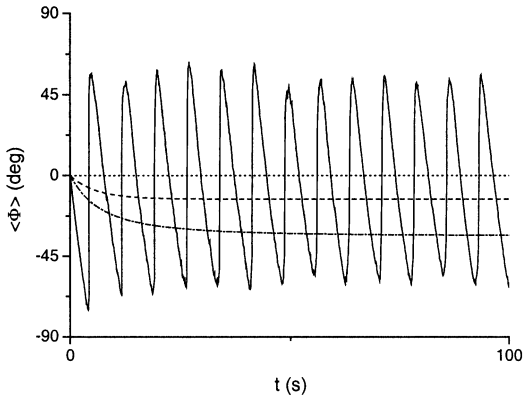

FIGURE 4 Average angle $\langle\Phi\rangle$ versus time for a PP sample. Dotted line corresponds to $\Omega = 0$; dashed line corresponds to $\Omega = \Omega_c/2$; dotted-dashed line corresponds to $\Omega = \Omega_c$; full line corresponds to $\Omega = 5\Omega_c$.

Downloaded by [University of Haifa Library] at 10:59 11 August 2012

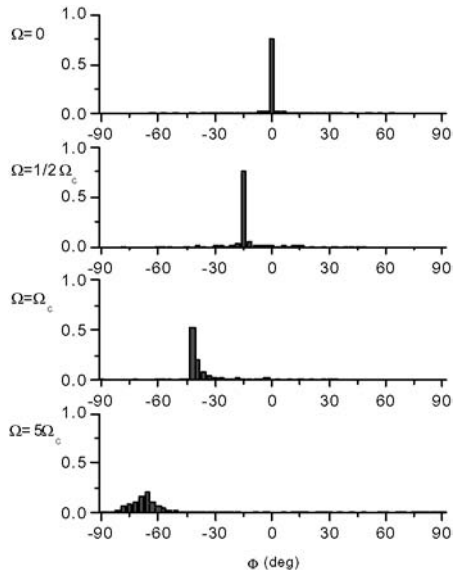

FIGURE 5 Histograms distributions of polar angle Φ for a PP sample at velocities $\Omega = 0$; $\Omega = \Omega_c$; $\Omega = \Omega_c$(stationary) and $\Omega = 5\Omega_c$ (at 100 s).

velocity. In case (c) the distribution is not stationary and is shown for $t = 100$s.

Escaped Radial (ER) Case

In the case of an ER generated sample (in the following simply ER case) the time evolution of the system is complicated by the presence of torques, which, from the beginning, are capable of affecting dynamically the director component along the rotation axis. In Figure 6 we show snapshots for the director patterns obtained for $\Omega = \Omega_c/2$ (a), $\Omega = \Omega_c$ (b), $\Omega = 5\Omega_c$ (c) at 50, 250 and 500 s. In all cases the sample central region, which is initially almost completely aligned with the cylinder axis, maintains its configuration for the whole simulation time, albeit its range is progressively confined to a smaller area surrounding the central point. Stationary distributions are apparently always reached, with helicoidally shaped patterns, but for higher velocities (c) the system goes through a transient oscillatory regime before arriving to a steady state.

Average angles $\langle\Theta\rangle$ and $\langle\Phi\rangle$ are shown in Figure 7. Again the case at zero rotational velocity is included for comparison. The following observations

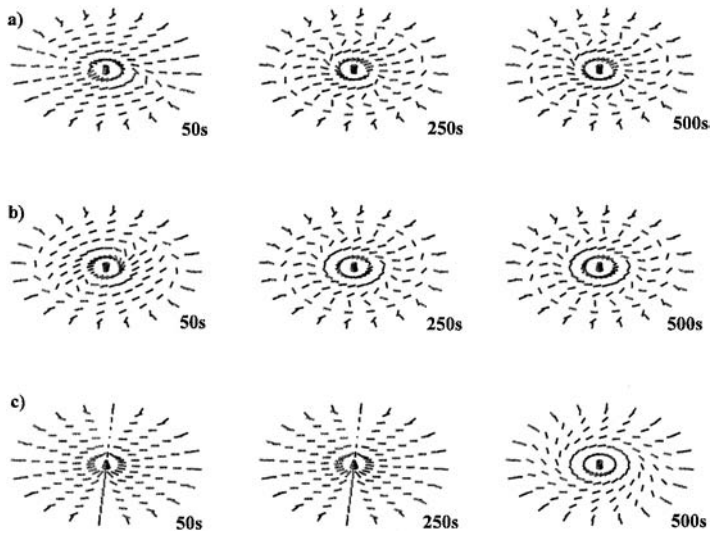

FIGURE 6 3-D snapshots of the director orientation for an ER sample, at velocities $\Omega = \Omega_c/2$ (a); $\Omega = \Omega_c$ (b) and $\Omega = 5\Omega_c$ (c).

Downloaded by [University of Haifa Library] at 10:59 11 August 2012

are easily made: first of all the sample tends to assume, on the average, an almost planar configuration, as it is shown by the average polar angle $\langle\Theta\rangle$, which goes to a limiting value close to 90°, i.e. the director tends to assume a planar configuration except for the central region, and increasingly so with increasing rotational velocity (the limiting value of Θ going from 85° at $\Omega = 0$ to 88° at $\Omega = 5\Omega_c$); the average azimuthal angle shows a different *transient* behaviour for velocity values smaller than the critical velocity, when it goes through a minimum value ranging from −15° (at $\Omega = \Omega_c/2$) to −20° (at $\Omega = \Omega_c$), to assume a stable value around −7°. In case (c), for a velocity much higher than the critical velocity, damped oscillations are observed with a period similar to the one predicted by the standard theory (around 6.5 s), and again a stationary value is reached close to zero. Notice that the slight noise observed in the diagrams is presumably due to numerical reasons, i.e. the finite precision of the integration algorithm resulting from the limited grid affects slightly the average at each time point. Histogram distributions, shown in Figure 8, for angles Φ and Θ and in Figure 9 for the director-field angle Φ_B in stationary conditions, give us complementary information to the average angle diagrams. If the distribution of polar angle Θ is practically independent from the rotational velocity, and mainly centred on 90°, with a small tail of reducing importance with increasing rotational velocity, azimuthal angle Φ takes an

Downloaded by [University of Haifa Library] at 10:59 11 August 2012

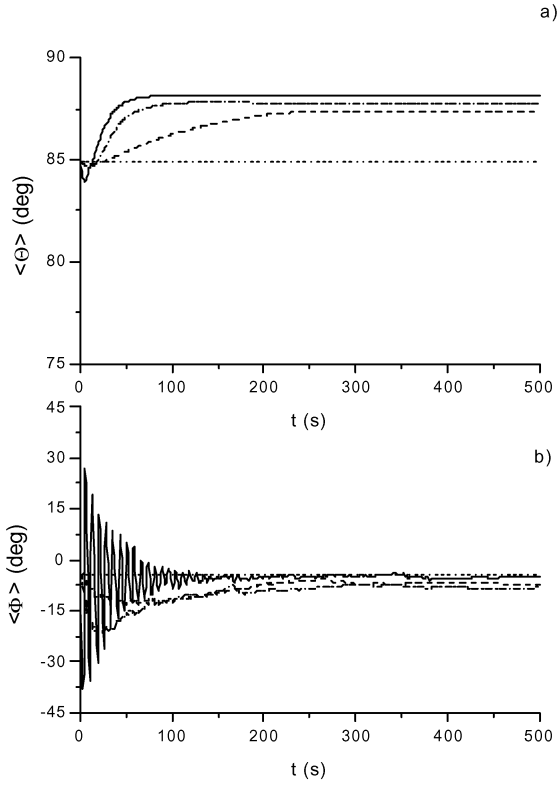

FIGURE 7 Average angles $\langle\Phi\rangle$ (a) and $\langle\Phi\rangle$ (b) versus time for an ER sample. Dotted line corresponds to $\Omega = 0$; dashed line corresponds to $\Omega = \Omega_c/2$; dotted-dashed line corresponds to $\Omega = \Omega_c$; full line corresponds to $\Omega = 5\Omega_c$.

increasingly spread distribution which becomes practically isotropic at higher velocities; angle Φ_B reflects the same behaviour.

CONCLUSIONS

The formation of director patterns in a rotating cylindrical nematic sample in the presence of a magnetic field perpendicular to the rotation axis has been analysed solving numerically three-dimensional LE equations for the director time evolution, combined with the assumption of stationary Newtonian velocity. The director patterns behaviour is rationalised assuming that initial defects, boundary conditions and time evolution imposed by sample rotation and magnetic torque act almost independently, contributing

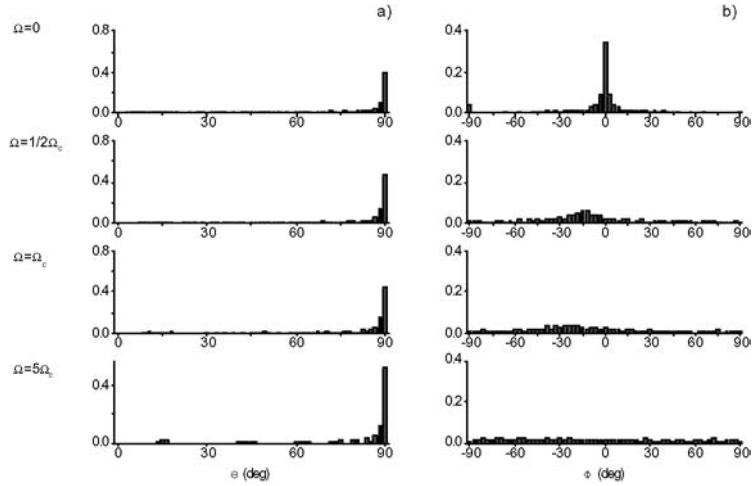

FIGURE 8 Stationary histograms distributions of angles Θ (a) and Φ (b) for an ER sample at velocities $\Omega = 0$; $\Omega = \Omega_c/2$; $\Omega = \Omega_c$ and $\Omega = 5\Omega_c$.

to the formation of space distributions that are not homogeneous in space, as predicted by simple previous analysis [1,2]. The role of the critical velocity parameter Ω_c as a discriminating number between stationary and

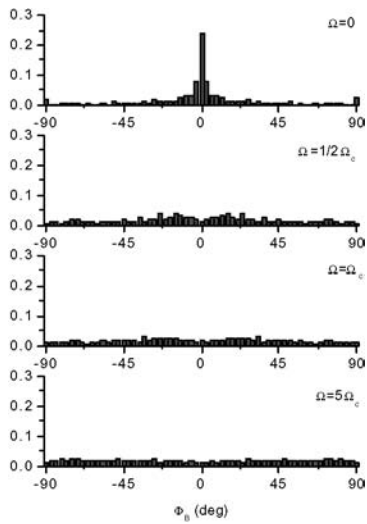

FIGURE 9 Stationary histograms distributions of director-field angle Φ_B for an ER sample at velocities $\Omega = 0$; $\Omega = \Omega_c/2$; $\Omega = \Omega_c$ and $\Omega = 5\Omega_c$.

Downloaded by [University of Haifa Library] at 10:59 11 August 2012

un-stationary patterns is weakened as far as the local distribution in space of the director is considered, although when averages of the director orientations extended to the whole sample are considered, it is still a significant measurement of the director dynamics. Out-of-plane director orientations tend to be naturally avoided due to the in-plane magnetic torque, but unstable central defects are persistent in time and cause a damped oscillating behaviour of the director average orientation in the sample.

It can be noted that damped director oscillations qualitatively analogous to those calculated in our ER case at high rotational velocity, have been observed in ESR [24] experiments, although in connection with an additional modulation which is not reproduced in the simulations reported here. Clearly, the director dynamics based on the simplified model presented here is an idealised description of the actual hydrodynamic behaviour of a rotating nematic. For high values of the imposed angular velocity, typical of sudden rotation experiments, the influence of the director distribution on the velocity field dynamics cannot be neglected, i.e. backflow effects cannot be excluded like in the present study. Moreover, the development of initial metastable director distributions is strongly influenced by thermal fluctuations, which have been neglected here. Nevertheless our simple analysis shows that even within the limit of classical hydrodynamic theory the director behaviour in three-dimension of a nematic fluid in set-ups currently employed for rheological, rheo-NMR and rheo-ESR experiments, can show surprising complexity, which can be rationalised only in the framework of a careful computational analysis, and should be taken into account in the interpretation of experimental findings.

Downloaded by [University of Haifa Library] at 10:59 11 August 2012

REFERENCES

[1] De Gennes, P. G. & Prost, J. (1993). *The Physics of Liquid Crystals*, 2nd Ed., Oxford University Press: Oxford.
[2] Chandrasekhar, S. (1992). *Liquid Crystals*, Cambridge University Press: Cambridge.
[3] Leslie, F. L. (1966). *Quart. J. Mech. Appl. Math*, *19*, 357; (1979). *Adv. Liq. Cryst.*, *4*, 1.
[4] Ericksen, J. L. (1961). *Trans. Soc. Rheolo.*, *5*, 23; (1976). *Adv. Liq. Cryst.*, *2*, 233.
[5] Rey, A. D. (1991). *J. Non-newtonian Fluid Mech.*, *40*, 177.
[6] Kneppe, H., Schneider, F., & Schwesinger, B. (1991). *Mol. Cryst. Liq. Cryst.*, *205*, 9; Heuer, H., Kneppe, H., & Schneider, F. (1991). *Mol. Cryst. Liq. Cryst.*, *200*, 51.
[7] Baleo, J. N., Vincent, M., Navard, P., & Demay, Y. (1992). *J. Rheol.*, *36*, 663.
[8] Han, W. H. & Rey, A. D. (1993). *J. Non-newtonian Fluid Mech.*, *50*, 1; (1993). *J. Non-newtonian Fluid Mech.*, *48*, 181; (1994). *J. Rheol.*, *38*, 1317; (1994). *Phys. Rev.*, *50*, 1688; (1994). *Phys. Rev.*, **49**, 597.
[9] Potze, W. & Heynderickx, I. (1995). *J. Non-newtonian Fluid Mech.*, *59*, 173.
[10] Chan, P. K. & Rey, A. D. (1997). *Liq. Cryst.*, *23*, 677.
[11] Chono, S., Tsuji, T., & Denn, M. M. (1998). *J. Non-newtonian Fluid Mech.*, *79*, 515.
[12] Chan, P. K. (1999). *Liq. Cryst.*, *26*, 1777; (2001). *Liq. Cryst.*, *28*, 207.
[13] Berry, G. C. & Srinivasarao, M. (1991). *J. Stat. Phys.*, *62*, 5–6, 1041.

[14] Burghardt, W. R. & Fuller, G. C. (1991). *Macromolecules*, *24*, 9, 2546.
[15] Larson, R. G. & Doi, M. (1991). *J. Rheol.*, *35*, 539.
[16] Marrucci, G. (1991). *Macromolecules*, *24*, 4176; (1991). *Phys. Scr.*, *T35*, 44.
[17] Chang, R. Y., Shiao, F. C., & Yang, W. L. (1994). *J. Non-newtonian Fluid Mech.*, *55*, 1.
[18] Fodor, J. S. & Hill, D. A. (1994). *J. Rheol.*, *38*, 1071.
[19] Muller, J. A., Stein, R. S., & Winter, H. H. (1994). *Rheol. Acta*, *33*, 473.
[20] Bajc, J., Hillig, G., & Saupe, A. (1997). *J. Chem. Phys.*, *106*, 7372.
[21] Mather, P. T. et al. (1997). *Rheol. Acta*, *36*, 485.
[22] Ignes-Mullol, J. & Shwartz, D. K. (2001). *Nature*, *410*, 348.
[23] Tsevtkov, V. & Sosnowskii, A. (1943). *Acta Physiochem. USSR*, *18*, 358.
[24] Leslie, F. M., Luckhurst, G. R., & Smith, H. J. (1972). *Chem. Phys. Lett.*, *13*, 368.
[25] Emsley, J. W., Khoo, S. K., Lindon, J. C., & Luckhurst, G. R. (1981). *Chem. Phys. Lett.*, *77*, 609.
[26] Kneppe, H. & Schneider, F. (1984). *J. Phys. E.*, *16*, 512.
[27] Martins, A. F., Esnault, P., & Volino, F. (1986). *Phys. Rev. Lett.*, *57*, 1745; Esnault, P., Casquilho, J. P., Volino, F., Martins, A. F., & Blumstein, A. (1990). *Liq. Cryst.*, *7*, 607; Casquilho, J. P., Gonçalves, L. N., & Martins, A. F. *Liq. Cryst.*, *21*, 651 (1996). Veron, A., Gomes, A. E., Leal, C. R., Van der Klink, J., & Martins, A. F. (1999). *Mol. Cryst. Liq. Cryst.*, *331*, 2359.
[28] Polimeno, A. & Martins, A. F. (1998). *Liq. Cryst.*, *25*, 5, 545; Polimeno, A., Martins A. F., & Nordio, P. L. (1999). *Mol. Cryst. Liq. Cryst.*, *328*, 541; Polimeno, A., Orian, L., Nordio, P. L., & Martins, A. F. (1999). *Mol. Cryst. Liq. Cryst.*, *336*, 17.
[29] Polimeno, A., Orian, L., Gomes, A. E., & Martins, A. F. (2000). *Phys. Rev. E.*, *62*, 2288; Martins, A. F., Gomes, A. E., Polimeno, A., & Orian, L. (2000). *Phys. Rev. E.*, *62*, 2301.
[30] Bird, R. B., Stewart, W. E., & Lightfoot, E. N. (1960). *Transport Phenomena*, Wiley: Chap. 3.
[31] Dunn, C. J., Ionescu, D., Kunimatsu, N., Luckhurst, G. R., Orian, L., & Polimeno, A. (2000). *J. Phys. Chem. B*, *104*, 10989.
[32] Cladis, P. E. & Kléman, M. (1972). *J. Phys. (Paris)*, *33*, 591.
[33] Ondris-Crawford, R. J., Crawford, G. P., Doane, J. W., Žumer, S., Vilfan, M., & Vilfan, I. (1998). *Phys. Rev. E*, *48*, 3.

Downloaded by [University of Haifa Library] at 10:59 11 August 2012